UNSUPERVISED ROBUST CHANGE DETECTION ON MULTISPECTRAL IMAGERY USING SPECTRAL AND SPATIAL FEATURES*

RAFAEL WIEMKER, ANJA SPECK, DANIEL KULBACH,
HARTWIG SPITZER, JOHANN BIENLEIN

Universität Hamburg, II. Institut für Experimentalphysik
Mail: FB Informatik / KOGS, Vogt-Kölln-Str. 30, 22527 Hamburg, FRG
WWW: http://kogs-www.informatik.uni-hamburg.de/projects/Censis.html
E-mail: wiemker@informatik.uni-hamburg.de

ABSTRACT

Change detection is a central task for land cover monitoring by remote sensing. It uses multitemporal image data sets in order to detect land cover changes from spectral discrepancies.

This paper describes a change detection strategy which integrates various concepts in order to make change detection robust against varying recording conditions, to utilize additional spatial features from local neighborhoods, and to enable unsupervised change detection. We consider change detection as an *unsupervised classification problem* with the two classes 'Change' and 'NoChange'. The decision can be made using *Bayes Rule*, which minimizes the probability of error.

We have successfully applied the described change detection strategy both to simulated imagery and real remotely sensed multispectral image data. The result of our unsupervised iterative algorithm are binary images showing the locations of 'Change'-areas, and probability images giving the Bayesian probability of 'Change' versus 'NoChange' for each pixel.

1. INTRODUCTION

Change detection is a central task for all kinds of monitoring purposes. It uses multitemporal image data sets in order to detect land cover changes caused by short-term phenomena such as flooding and seasonal vegetation change, or long-term phenomena such as urban development and deforestation.

In particular, change detection based on remotely sensed multispectral images has developed into an important technique for a multitude of fields (Lillesand & Kiefer 1987, Singh 1989, Richards 1993). It supports research and monitoring in virtually all geosciences, as well as in cadastre, land use management and urban planning. It is widely applied in military reconnaissance, and more recently its benefits are also

*Presented at the Third International Airborne Remote Sensing Conference and Exhibition, 7–10 July 1997, Copenhagen, Denmark.

investigated for international confidence building by cooperative verification of arms control within the framework of the Open Skies Treaty (Wiemker & Spitzer 1996, Ryan et al. 1996, Spitzer et al. 1997).

In general, remotely sensed imagery for monitoring purposes is recorded by overflights over the same land area at two times, T_1 and T_2, say. An appropriate algorithm must then compare the two observed images of the same scene and assist the analyst by designating those areas where the ground cover has probably changed. For specific applications, certain wavelength bands may be selected, whereas for general purpose monitoring, all spectral bands will be taken into account.

A pre-requisite to pixel-wise change detection is the geometric *registration* between the two images to be compared. Registration can be carried out either by geocoding of both images or by direct image-to-image registration. A typical problem of multispectral imagery recorded with airborne line scanners is that the registration yields accuracies of some pixels at best. Even when the geometric position of the footprint of a certain pixel can be pinpointed to subpixel accuracy (*e.g.* by using coupled DGPS and inertial navigation system), still the displacement of elevated features (such as house or trees) must be taken into account. This displacement is caused by the varying flight tracks of aircraft (in contrast to satellites) and the usually large swath angles of airborne scanners which allow for oblique viewing angles. Therefore, imagery from airborne scanners in general requires locally adaptive coordinate transformation functions as described in previous efforts (Ehlers 1994, Wiemker 1996, Wiemker et al. 1996).

2. ROBUST CHANGE DETECTION BY ITERATIVE PRINCIPLE COMPONENT TRANSFORMATION

A fundamental problem of comparing two images of the same scene is that the recording conditions may have changed. Change detection techniques should be robust in that they should be invariant against atmospheric parameters and imaging parameters which could possibly have changed between the two recordings.

In particular, the direct solar illumination and the diffuse sky light, the path radiance, and the transmittance of the atmosphere, as well as the dark current and gain setting of the sensor may have changed individually in each spectral band. All these effects can roughly be categorized into influencing the received spectral signal in either a multiplicative or an additive way. Thus the relation between the spectral signal $x_i(T_1)$ and $x_i(T_2)$ received from a certain Lambertian reflecting surface at two times T_1 and T_2 is very often modeled approximately as a linear function (Richards 1993, Singh 1989).

Let us consider a bitemporal feature space for a single spectral band i where each pixel $\mathbf{x}$ is denoted by a point $\mathbf{x}_i = [x_i(T_1)\,,\, x_i(T_2)]^{\mathrm{T}}$ (Fig. 1, left). Then, as a consequence of the assumed linear relation between unchanged pixels, we expect all unchanged pixels to lie in a narrow elongated cluster along a principal axis. On the other hand, the pixels which do have experienced 'change' in their spectral appearance are expected to lie far away from this axis (Richards 1993). In other words, the magnitude of 'change' is quantified by the magnitude of the second principal component (PC): $c_i = \mathbf{e}_{2,i}^{\mathrm{T}}\,(\mathbf{x}_i - \mathbf{m}_i)$, where $\mathbf{e}_{2,i}$ is the second eigenvector of the overall covariance matrix $\mathbf{C}_i = \frac{1}{n}\sum_{\mathbf{x}}(\mathbf{x}_i - \mathbf{m}_i)(\mathbf{x}_i - \mathbf{m}_i)^{\mathrm{T}}$ (2×2 matrix) of spectral band i, and $\mathbf{m}_i = \frac{1}{n}\sum \mathbf{x}_i$ is the mean vector of all n vectors $\mathbf{x}_i$.

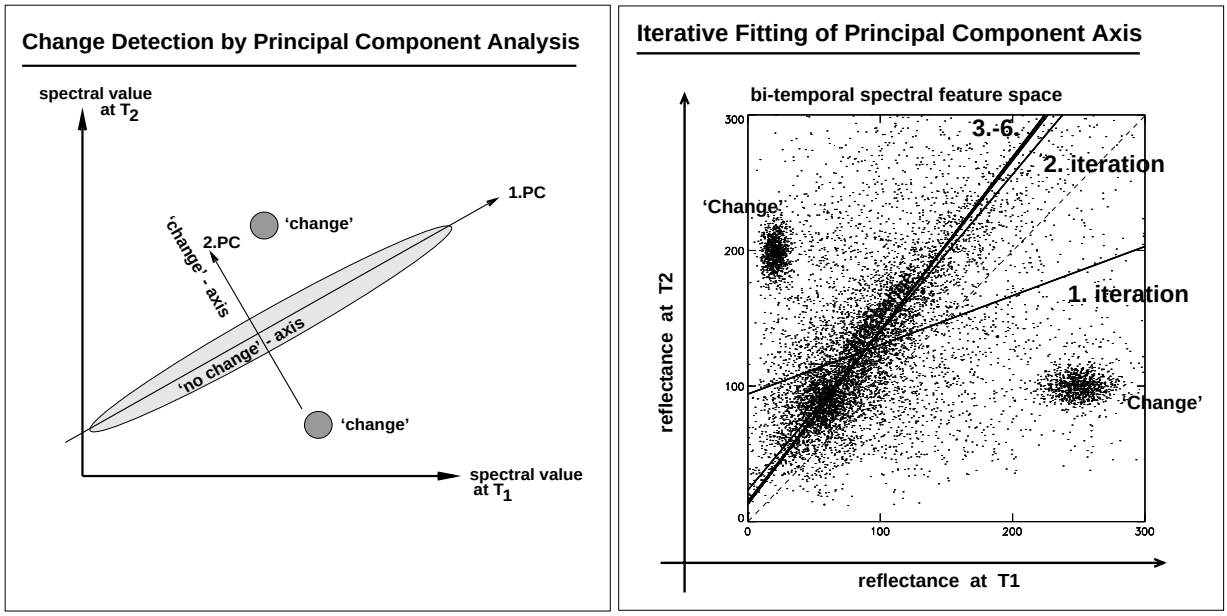

Figure 1: Left: Concept of 'Change'. Right: Iterative fitting of the 'NoChange'-axis. The data points stem from real scanner imagery taken over an urban area, superimposed with noise and simulated 'Change'-areas.

An obvious problem with principal component based change detection is that the principal components are conventionally estimated as the eigenvectors of the covariance matrix $\mathbf{C}_i$ which is computed from *all* pixels $\mathbf{x}_i$, including those which have experienced 'change'. Thus the such found 'NoChange'-axis is prone to error (see the first iteration in Fig. 1, right). In our iterative approach the problem is addressed such that the cluster mean and the covariance matrix are re-computed from all pixels but this time weighted with their respective probabilites to be 'NoChange'-pixels. This is repeated and converges after only a few iterations to a final position of the 'NoChange'-axis (Fig. 1, right).

3. UTILIZING SPATIAL NEIGHBORHOOD FEATURES

In addition to purely spectral features we want to consider spatial features. After all, spatial relations are the defining quality of an image as such. We use several ways by which we let spatial features influence the change detection process.

Firstly, for each pixel $\mathbf{x}$ we consider its spatial neighborhood $\mathcal{N}(\mathbf{x})$ and determine the local variance $\sigma_i^2(\mathbf{x}) = \sum_{\mathbf{x}' \in \mathcal{N}(\mathbf{x})} (x_i' - \widehat{x}_i)^2 / (k^2 - 1)$ in spectral band i, where $\widehat{x}_i$ is the mean value in the neighborhood, and $(k^2 - 1)$ is the number of pixels in the local neighborhood which we define as the quadrangular $k \times k$ window around the center pixel. The local variance of both recording times is combined into $\sigma_i^2(\mathbf{x}) = \sigma_i^2(\mathbf{x}, T_1) + \sigma_i^2(\mathbf{x}, T_2)$. When fitting the principal component vectors, the feature space points $\mathbf{x}$ are weighted inverse to the square root of their local variance in order to account for the estimated accuracy of their respective spectral value. *I.e.*, pixels in homogeneous neighborhoods will have larger weight than those in an inhomogeneous area.

Secondly, the spectral change component c_i, *i.e.*, the deviation of the point $\mathbf{x}_i = [x_i(T_1)\,,\; x_i(T_2)]^{\mathrm{T}}$ from the 'NoChange'-axis in the bitemporal feature space, is being set in relation to the local variance $\sigma_i^2(\mathbf{x})$. This prevents image areas which exhibit high spatial frequencies from being prone to erroneous change detection such as caused by small misregistration errors. We therefore divide the change component by the square root of the local variance: $c_i(\mathbf{x})/\sigma_i(\mathbf{x})$.

Thirdly, we assume a positive spatial correlation: the probability of a pixel to belong to the 'Change'-class is encouraged or discouraged by the respective probabilites of the surrounding pixels in the local neighborhood. This can be achieved by simply smoothing the change components $c_i(\mathbf{x})$ in the image domain. Another way is to define a neighborhood potential which depends on the class memberships of neighboring pixels, and to derive proper spatial probabilities from Markov random field modeling (*e.g.* the ICM algorithm (Besag 1986, Li 1995)). We achieved similarly encouraging results with both methods. The size of the local neighborhood and the magnitude of influence of the spatial versus spectral features can be tuned by the analyst with respect to specific applications (see Fig. 2, 3).

Our experience with real remotely sensed multispectral imagery has shown that the local variance $\sigma_i^2(\mathbf{x})$ around pixel $\mathbf{x}$ in spectral band i is in itself a powerful feature for change detection. Additionally to evaluating the discrepancy between the spectral values $x_i(T_1)$ and $x_i(T_2)$, it proved useful to consider also the discrepancy between the logarithms of the local variances at two recording times: $\ln \sigma_i^2(\mathbf{x}, T_1)$ vs. $\ln \sigma_i^2(\mathbf{x}, T_2)$. Per definition, *variances* are not influenced by any additive offset in the data such as path radiance or dark current, and are positive definite. Comparing the *logarithm* of the variance is convenient, as different scaling factors at the two recording times T_1 and T_2 are reduced to an additive offset which can be removed easily by subtracting the average of all such defined changes.

4. UNSUPERVISED CHANGE DETECTION AS A CLUSTERING PROBLEM

Considering multispectral images with N spectral bands yields an N-dimensional change space, as spectral 'change' c_i can occur independently in each spectral band in a positive or negative direction. The overall *magnitude of change* (or *degree of change*) can be evaluated by summing up the squared spectral changes: $\sum_{i=1}^{N} c_i^2/N$. For specific applications one may want to apply weights w_i in order to emphasize particular spectral bands: $\sum_i w_i c_i^2 / \sum_i w_i$. Usually the analyst will define a threshold, either for the change component c_i in a specific spectral band i or for the overall magnitude of change, in order to produce a 'Change' vs. 'NoChange' binary image.

Alternatively to interactive thresholding, we developed an *unsupervised* approach which considers change detection as a classification problem, where each pixel is assigned to one out of two classes: 'Change' or 'NoChange'. The decision can be made using *Bayes Rule*, which minimizes the probability of error (Duda & Hart 1973). The Bayesian decision is based on the spectral and spatial features (as described above) and Gaussian probability densities which are estimated iteratively for both the 'Change' and the 'NoChange' class.

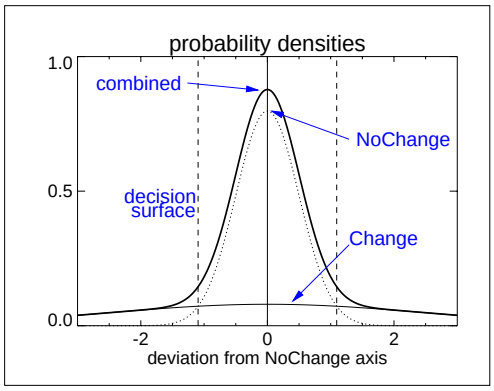

The iteration starts by assigning equal probabilitites of 0.5 for 'Change' and 'NoChange' to each pixel. Symmetry is broken by the differing distances to the iteratively fitted 'NoChange'-axis. The sensitivity for finding 'Change' can be tuned by setting *a priori* 'Change'- and 'NoChange'-probabilitites. After convergence, the algorithm produces a binary image with the Bayesian decision for 'Change' or 'NoChange', and two probability images which contain the respective probabilities of each pixel for both classes. It thus delivers error probabilities for first kind of error (undetected true 'Change') and second kind (mislabeled true 'NoChange').

The unsupervised clustering process can iterate using all N spectral bands 'simultaneously'. Then a pixel currently identified as 'changed' in a particular spectral band will also be weighted as such in another spectral band, even if it lies close to the 'NoChange'-axis there. The 'simultaneous' iteration is theoretically more satisfactory, even though separated iteration processes in each spectral band are computationally much faster.

5. CHANGE DETECTION RESULTS AND VISUALIZATION IN THE HSV COLOR SPACE

We have applied the described change detection strategy to simulated test imagery and real multispectral image data in supervised (Speck 1997) and unsupervised mode. The codes were written in the IDL / PVWAVE interpreter languages, and are currently being integrated into the ENVI remote sensing image processing environment. The imagery was recorded by a DAEDALUS AADS 1268 line scanner with $N = 10$ spectral bands during four campaigns from 1991 to 1995 in cooperation with the German Aerospace Research Establishment (DLR) at flight altitudes of 300 m and 1800 m (nadir ground resolution 70 cm and 4.2 m, respectively). The detected changes can be checked by eye appraisal against high resolving aerial photography and show promising results. Fig. 2 and 3 show two examples of detected changes.

For visualization of the detected changes between two multispectral images we have found it most useful to employ the Hue-Saturation-Value (HSV) color system. The HSV color system is described *e.g.* by Foley et al. (1995). We substitute the overall magnitude of change $\sum_{i=1}^{N} c_i^2/N$ as the color saturation value for each pixel in the final 'change'-image: areas of low magnitude of 'change' then have vanishing saturation and thus appear white or gray.

Then, for each pixel, the particular spectral band is identified which carries the maximum fraction of the overall magnitude of change for this pixel. Each of the N spectral bands is coded with a discrete color hue. The hue of the maximally contributing spectral band is assigned to the pixel in question.

In an alternative usage of the color hue, the N-dimensional change space is projected onto its two most significant principal component vectors $\mathbf{e}_1$ and $\mathbf{e}_2$ and thus transformed into new principal component coordinates e_1 and e_2. Experience has shown that the 'change' c_i is highly correlated through the N spectral bands, and that the two most significant principal components e_1 and e_2 can capture ca. 90% of the overall variance of the change space. We then take the phase angle $\phi = \arctan(e_2/e_1)$ between the principal components to get a color hue value out of the color cycle (0° red, 120° green, 240° blue). Thus areas of different spectral change characteristic appear coded with different color hues in the final 'change'-image.

Finally, for better topographic orientation, one spectral band of either one of the compared original images is histogram-equalized and employed as the intensity value for each pixel. Then to the analyst it is immediately apparent which image objects are lying within the colored 'Change'-patches. Finally, the HSV-image is converted to an RGB-'true color'-image and displayed.

6. CONCLUSIONS

In summary, we have found that:

- Iterative principle component transform converges fast to a robust 'NoChange'-axis which is invariant against additive offsets and scaling factors which may possibly vary between the recording times.
- Weighting the spectral 'Change'-component inversely with the local spectral variance suppresses spurious 'Change'-results in high texture areas.
- The local spectral variance also is a powerful feature in its own right for detecting changes, and per definition invariant against additive offsets such as path radiance and detector dark current. Objects of a size smaller then the window size used for estimation of the local variance are detected successfully.
- Utilizing spatial correlation improves the results significantly, both with mechanisms derived from Markov random field modeling (neighborhood potential) or from simple image smoothing operations.
- Unsupervised clustering algorithms can be employed successfully in the change space as spanned by the 'Change'-components from N spectral bands and deliver convincing results. It remains important for the analyst, however, to be able to tune the sensitivity of the change detection process and to select application specific wavelength bands.
- The HSV color space is very useful for screen display of change detection results, where the color *saturation* indicates the magnitude of change, the color *hue* the spectral characteristic, and the *intensity* one of the underlying original images (for illustration, some color 'Change'-images are appended to the postscript-version of this paper which can be downloaded from our WWW-site: `http://kogs-www.informatik.uni-hamburg.de/projects/censis/publications.html`).

ACKNOWLEDGEMENT

This work was supported by the Volkswagen-Stiftung, Hannover. We would like to thank Martin Kollewe and Thomas Kollewe for inspiring discussions and the organization of the image flights which were conducted in collaboration with the German Aerospace Research Establishment (DLR), Oberpfaffenhofen, particularly with the help of Volker Amann, Peter Hausknecht and Rudolf Richter.

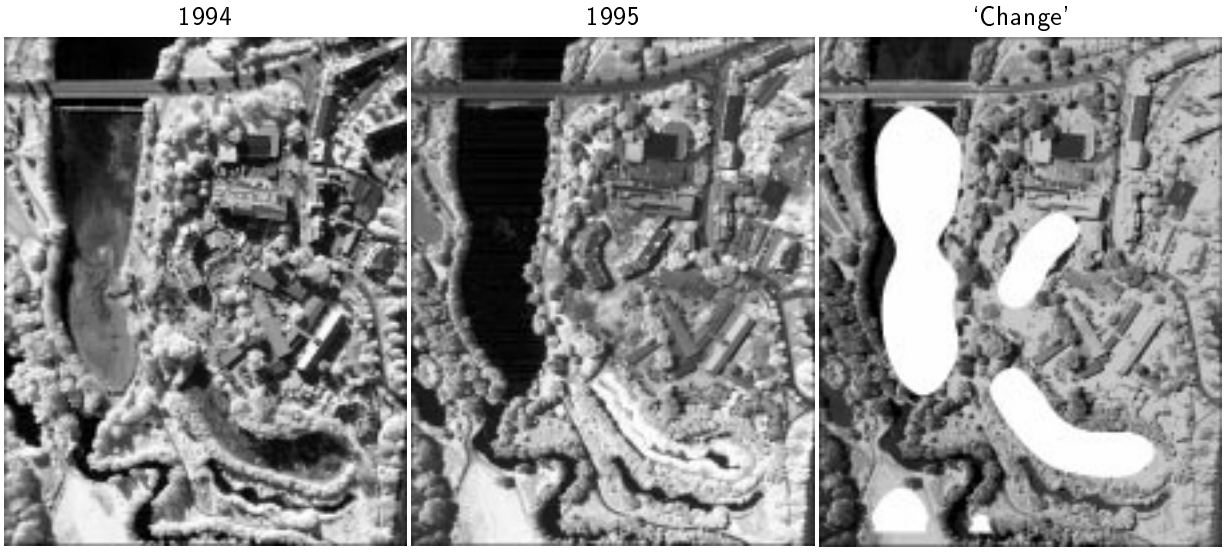

Figure 2: 'Change'-image (right, 800×650 pixels) as detected from iterative principal component analysis, considering a large local neighborhood of 45×45 pixels. 'Change'-areas are whitened.

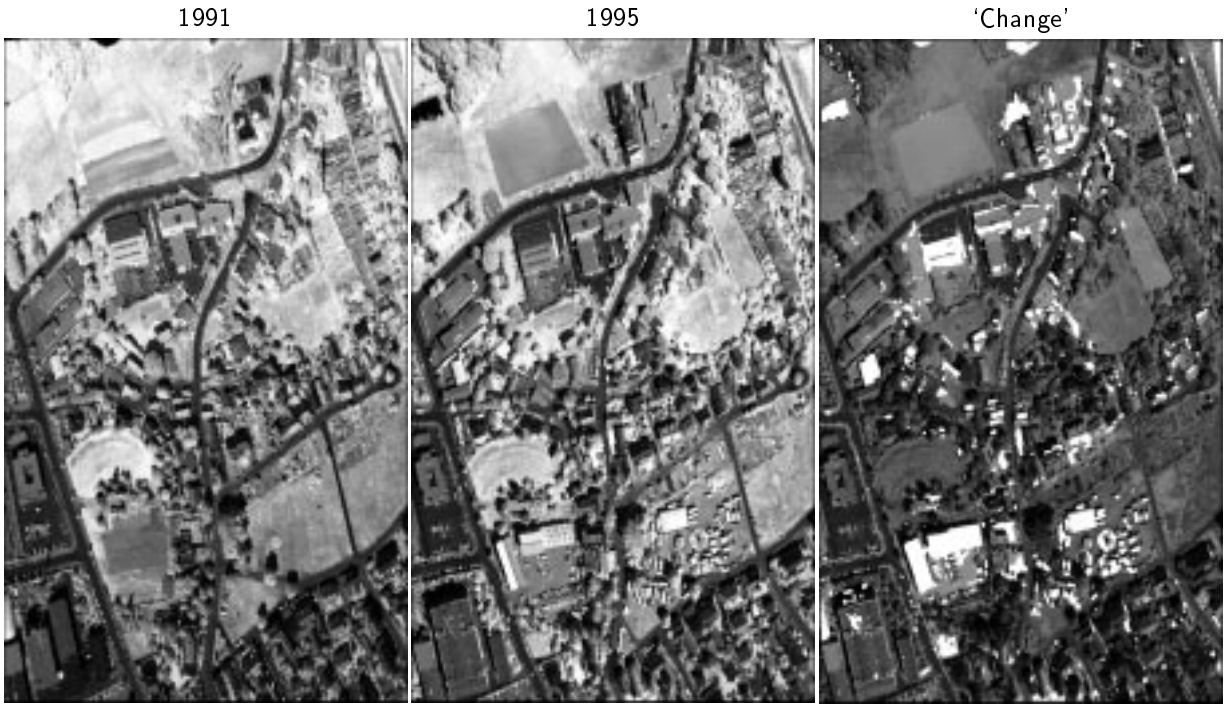

Figure 3: 'Change'-image (right, 900×550 pixels) as detected considering a small local neighborhood of 5×5 pixels. 'Change'-areas are whitened.

REFERENCES

Besag, J. (1986). On the statistical analysis of dirty pictures. *Journal of the Royal Statistical Society B* **48** (3), 259–302, 1986.

Duda, R. O. and P. E. Hart (1973). *Pattern Classification and Scene Analysis*. Wiley, New York, 1973.

Ehlers, M. (1994). Geometric Registration of Airborne Scanner Data Using Multiquadric Interpolation Techniques. In *Proceedings of the First International Airborne Remote Sensing Conference and Exhibition, Strasbourg*, Ann Arbor, 1994, volume II, pages 492–502. Environmental Research Institut of Michigan.

Foley, J., A. Van Dam, S. Feiner, and J. Hughes (1995). *Computer Graphics: Principles and Practice*. Addison-Wesley, Reading, MA, 1995.

Li, S.Z. (1995). *Markov Random Field Modeling in Computer Vision*. Springer, Tokyo, 1995.

Lillesand, T.M. and R.W. Kiefer (1987). *Remote Sensing and Image Interpretation*. Wiley, New York, 1987.

Richards, J. A. (1993). *Remote Sensing Digital Image Analysis*. Springer, Heidelberg, New York, 1993.

Ryan, R., P. Del Guidice, L. Smith, M. Soel, N. Fonneland, M. Pagnutti, R. Irwin, and P. Saatzer (1996). U.S. Open Skies Follow-On Sensors Evaluation Program, Multispectral Hyperspectral (MSHS) Sensor Survey. In *Proceedings of the Second International Airborne Remote Sensing Conference and Exhibition, San Francisco*, Ann Arbor, 1996, volume I, pages 392–402. Environmental Research Institut of Michigan.

Singh, A. (1989). Review Article: Digital change detection techniques using remotely-sensed data. *International Journal of Remote Sensing* **10** (6), 989–1003, 1989.

Speck, A. (1997). Änderungsdetektion auf multispektralen Luftbildern durch Hauptachsentransformationen im bitemporalen Merkmalsraum, 1997. Diplomarbeit, Universität Hamburg, II. Institut für Experimentalphysik, CENSIS-Report 26-97.

Spitzer, H., R. Wiemker, A. Speck, and J. Bienlein (1997). Robuste unbeaufsichtigte Änderungsdetektion auf Multispektralbildern im Rahmen des Open-Skies-Vertrages. In Altmann, J. and G. Neuneck, editors, *Naturwissenschaftliche Beiträge zu Abrüstung und Verifikation, Verhandlungen der Fachsitzung der 61. Physikertagung der Deutschen Physikalischen Gesellschaft (DPG) in München 1997*. DPG / FONAS (Math.Seminar, Bundesstr. 55, D-20146 Hamburg), 1997. In print.

Wiemker, R. and H. Spitzer (1996). Änderungsdetektion auf multispektralen Luftbildern – Perspektiven für den Open-Skies-Vertrag. In Altmann, J. and G. Neuneck, editors, *Naturwissenschaftliche Beiträge zu Abrüstung und Verifikation, Verhandlungen der Fachsitzung der 60. Physikertagung der Deutschen Physikalischen Gesellschaft (DPG) in Jena 1996*, pages 138–151. DPG / FONAS (Math.Seminar, Bundesstr. 55, D-20146 Hamburg), 1996.

Wiemker, R., K. Rohr, L. Binder, R. Sprengel, and H.S. Stiehl (1996). Application of Elastic Registration to Imagery from Airborne Scanners. In *Proceedings of the XVIII. Congress of the International Society for Photogrammetry and Remote Sensing ISPRS 1996, Vienna*, volume XXXI part B4 of *International Archives of Photogrammetry and Remote Sensing*, pages 949–954, 1996.

Wiemker, R. (1996). Registration of Airborne Scanner Imagery Using Akima Local Quintic Polynomial Interpolation. In *Proceedings of the Second International Airborne Remote Sensing Conference and Exhibition, San Francisco*, Ann Arbor, 1996, volume III, pages 210–219. Environmental Research Institut of Michigan.

'Change' visualization in the HSV color system

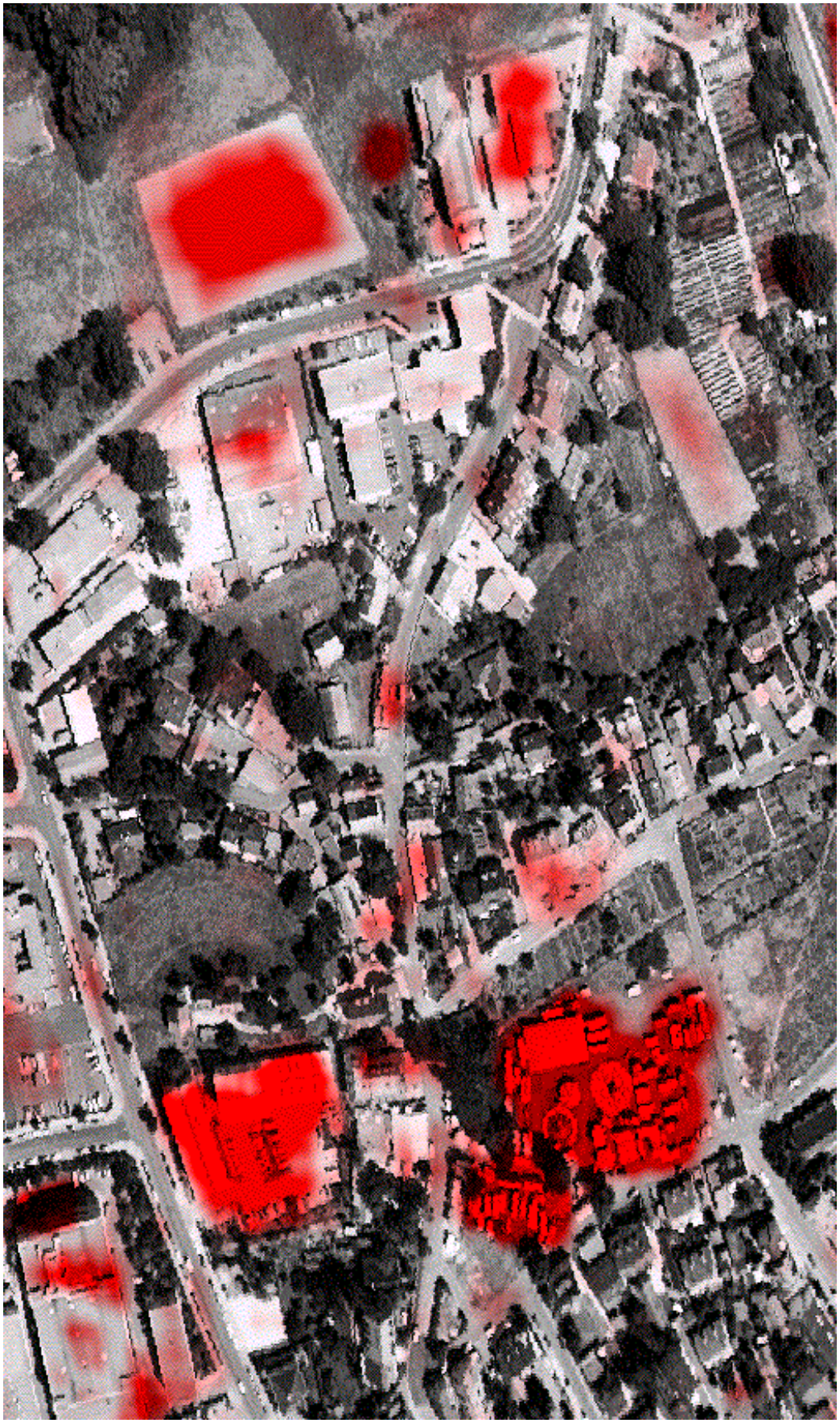

'Change'-image as detected from the temporal difference of logarithmic local variance, considering a larger local neighborhood of 15×15 pixels. The 'change'-hue is fixed to 'red', while the magnitude of 'change' is coded in the color saturation (*i.e.*, `NoChange' has vanishing saturation and thus appears white or gray); the intensity values stem from one band of the underlying images.

'Change' visualization in the HSV color system

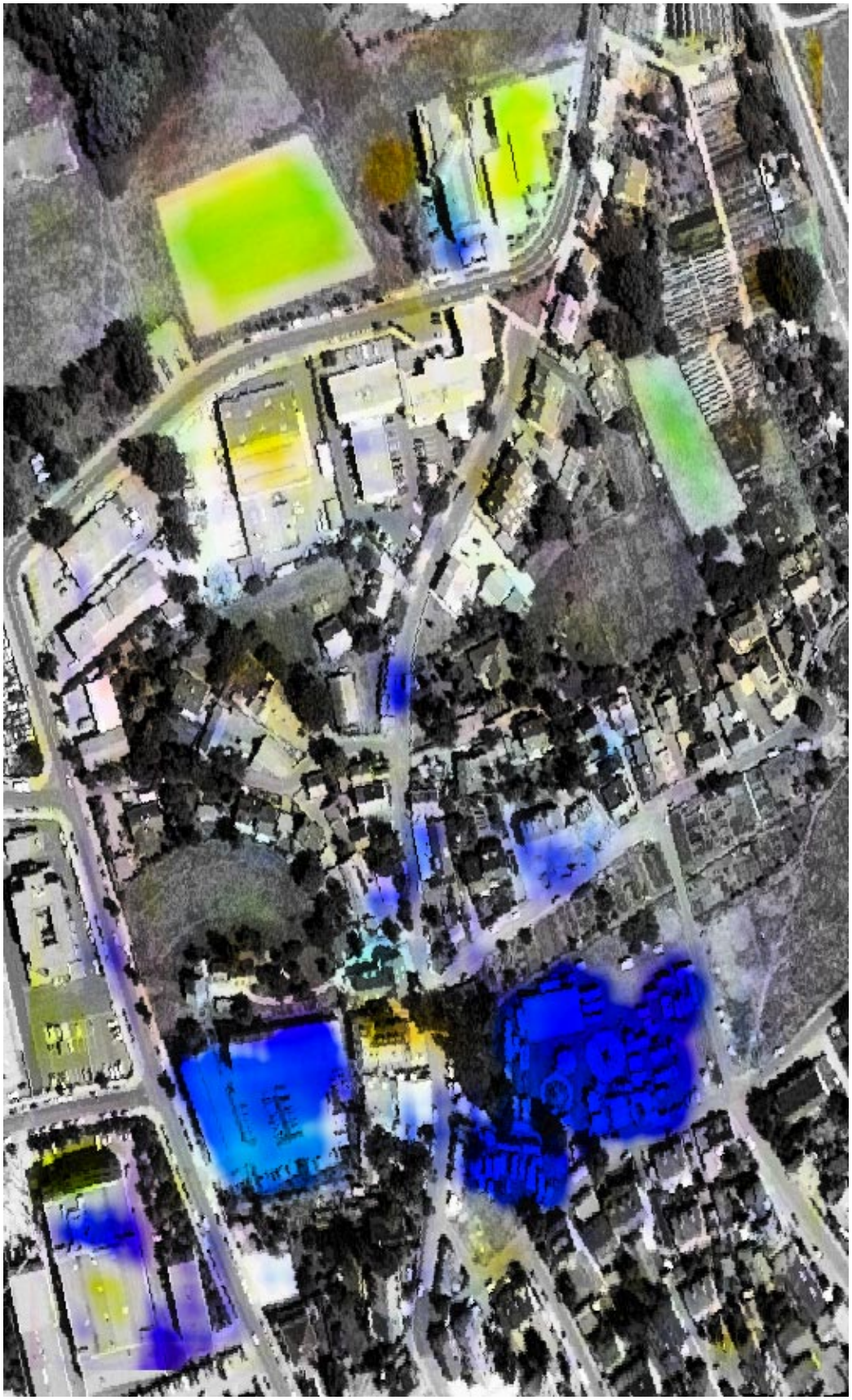

'Change'-image as detected from the temporal difference of logarithmic local variance, considering a larger local neighborhood of 15×15 pixels. The 'change'-hue codes the spectral 'direction' of change in the N-dimensional change space, while the magnitude of 'change' is coded in the color saturation (*i.e.*, `NoChange' has vanishing saturation and thus appears white or gray); the intensity values stem from one band of the underlying images.

'Change' visualization in the HSV color system

'Change'-image as detected from the temporal difference of logarithmic local variance, considering a small local neighborhood of 5×5 pixels. The 'change'-hue codes the spectral 'direction' of change in the N-dimensional change space, while the magnitude of 'change' is coded in the color saturation (*i.e.*, `NoChange' has vanishing saturation and thus appears white or gray); the intensity values stem from one band of the underlying images.

'Change' visualization in the HSV color system

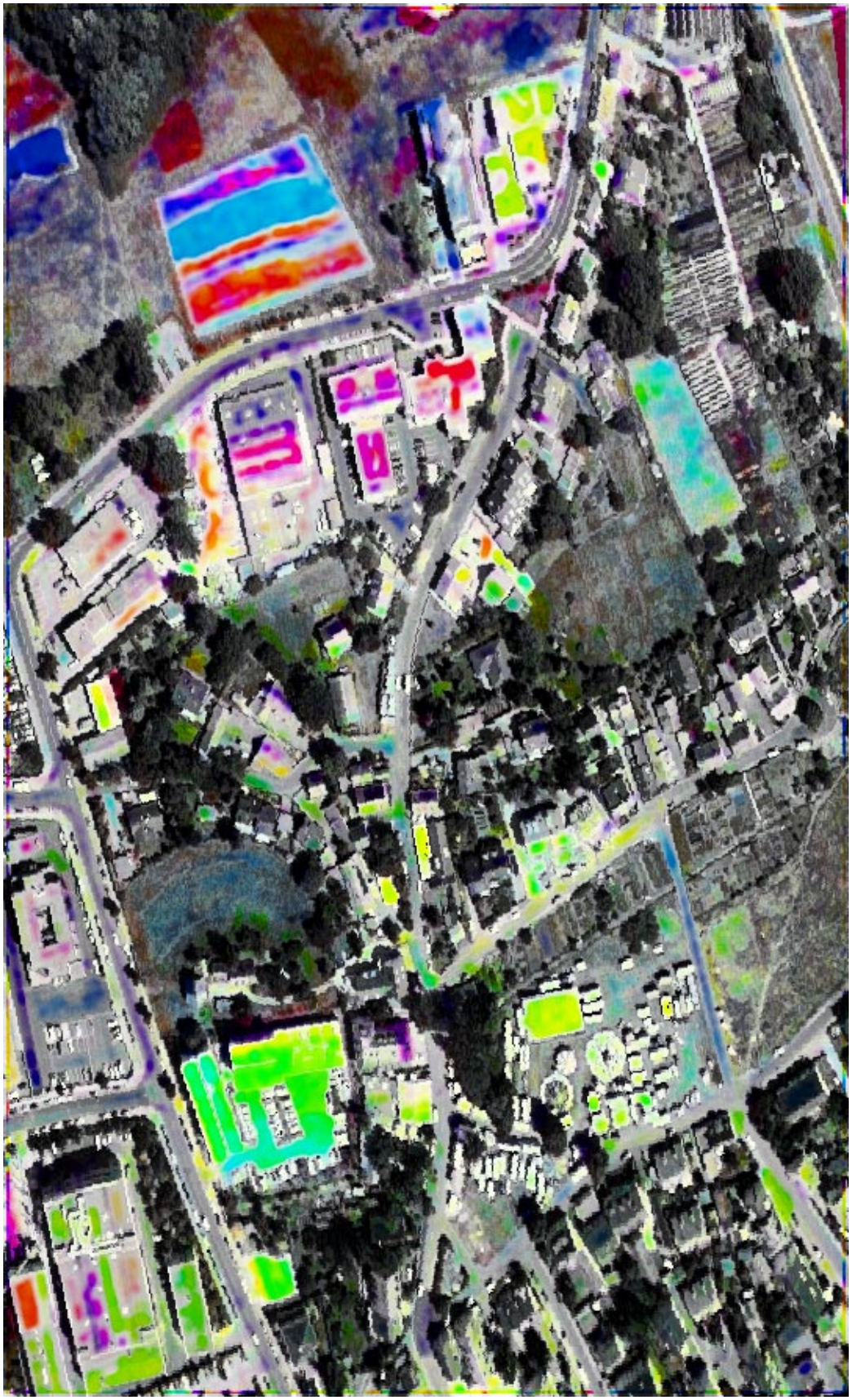

'Change'-image as detected from iterative principle component analysis (with local variance normalization c_i/σ_i), considering a small local neighborhood of 5×5 pixels. The 'change'-hue codes the spectral 'direction' of change in the N-dimensional change space, while the magnitude of 'change' is coded in the color saturation (*i.e.*, `NoChange' has vanishing saturation and thus appears white or gray); the intensity values stem from one band of the underlying images.

'Change' visualization in the HSV color system

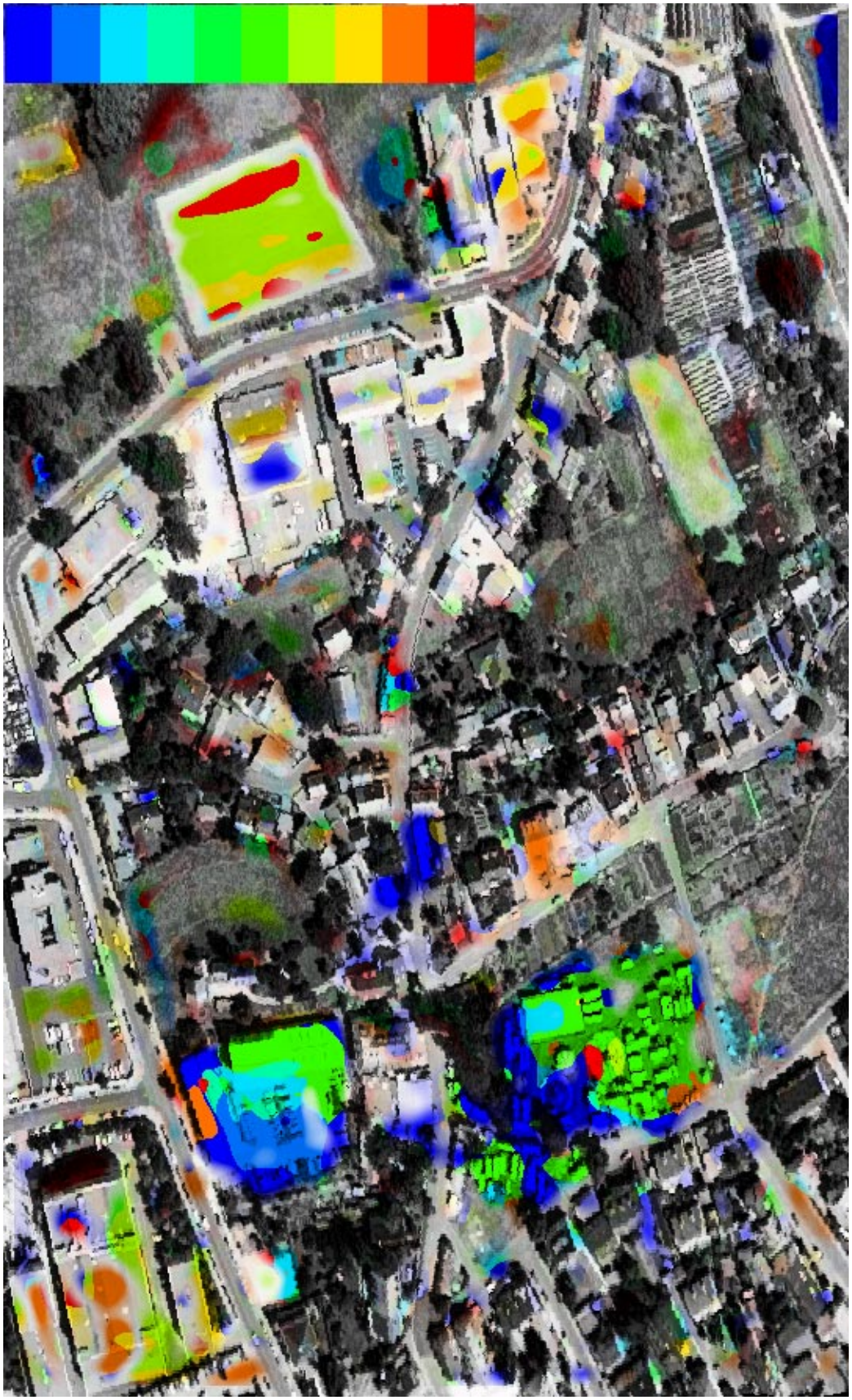

'Change'-image as detected from the temporal difference of logarithmic local variance, considering a larger local neighborhood of 15×15 pixels. The 'change'-hue indicates which of the 10 spectral bands carries the maximum 'change' (see the 10 color bars (top left) for comparison; blue: visible, green: near infrared, red, medium infrared), while the magnitude of 'change' is coded in the color saturation (*i.e.*, `NoChange' has vanishing saturation and thus appears white or gray); the intensity values stem from one band of the underlying images.

'Change' visualization in the HSV color system

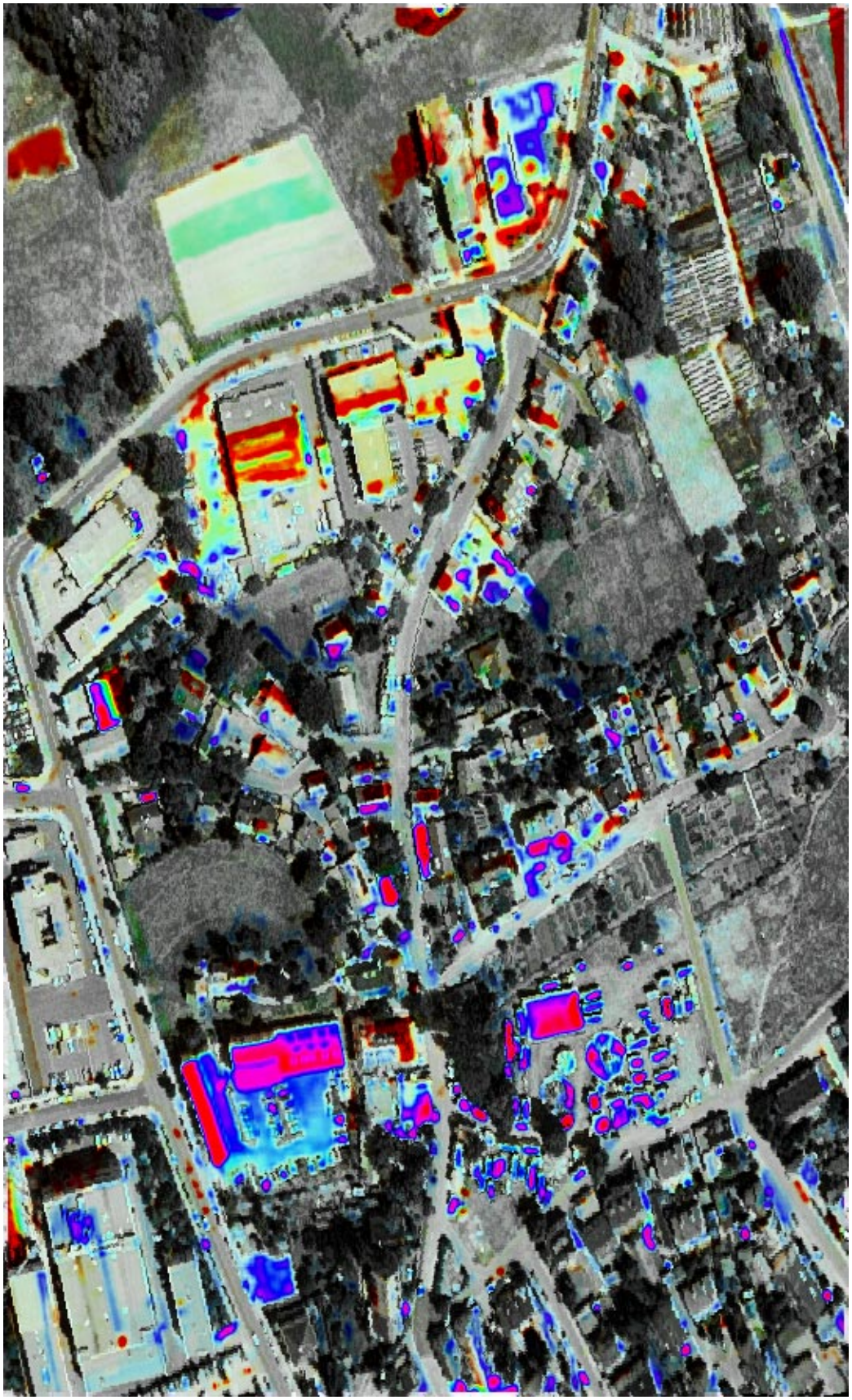

'Change'-image as detected from iterated principle component transform (without local variance normalization c_i/σ_i), considering a small local neighborhood of 5×5 pixels. The magnitude of 'change' is coded in the color saturation (*i.e.*, `NoChange' has vanishing saturation and thus appears white or gray); the 'change'-hue codes the direction of change $\sum_i c_i$ (albedo): red indicates a increased albedo, green neutral, and blue decreased albedo; the intensity values stem from one band of the underlying images.